

CADSpotting: Robust Panoptic Symbol Spotting on Large-Scale CAD Drawings

Jiazuo Mu^{1,2†} Fuyi Yang^{1,2†} Yanshun Zhang² Junxiong Zhang^{1,2} Yongjian Luo¹
 Lan Xu¹ Yujiao Shi¹ Jingyi Yu^{1‡} Yingliang Zhang^{2‡}
¹ ShanghaiTech University ² DGene Digital Technology

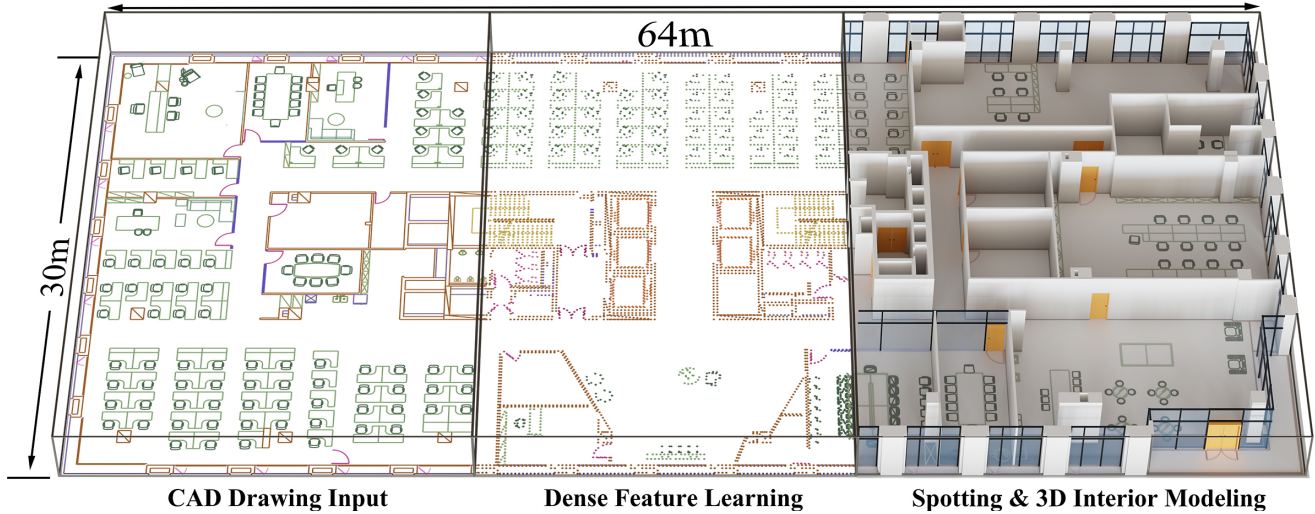


Figure 1. Our CADSpotting accurately identifies and segments symbols in CAD drawings, thereby enhancing the efficiency of tasks such as 3D interior modeling. The approach employs a dense point sampling method within a unified point cloud processing model to improve primitive feature representation. Additionally, a Sliding Window Aggregation technique is incorporated during inference to facilitate panoptic symbol spotting in large-scale CAD drawings.

Abstract

We introduce CADSpotting, an efficient method for panoptic symbol spotting in large-scale architectural CAD drawings. Existing approaches struggle with the diversity of symbols, scale variations, and overlapping elements in CAD designs. CADSpotting overcomes these challenges by representing each primitive with densely sampled points, described by essential attributes like coordinates and colors. Building upon a unified 3D point cloud model for joint semantic, instance, and panoptic segmentation, CADSpotting learns robust feature representations. To enable accurate segmentation in large, complex drawings, we further propose a novel Sliding Window Aggregation (SWA) technique, combining weighted voting and Non-Maximum Suppression

(NMS). Moreover, we introduce a large-scale CAD dataset named LS-CAD to support our experiments. Each floorplan in LS-CAD has an average coverage of 1,000 m² (versus 100m² in the existing dataset), providing a valuable benchmark for symbol spotting research. Experimental results on FloorPlanCAD and LS-CAD datasets demonstrate that CADSpotting outperforms existing methods, showcasing its robustness and scalability for real-world CAD applications.

1. Introduction

Architectural Computer-Aided Design (CAD) drawings, especially those used for interior design, serve as detailed digital representations that convey essential information about a building’s structure, layout, and intricate details. These drawings include critical elements such as furniture placement, electrical layouts, and spatial organization, ensuring consistency and precision throughout the construction process. For instance, the Shanghai Mercedes-Benz Arena uti-

† Equal contributions.
 ‡ Corresponding author.

lized over 3,000 CAD drawings to guide its structural design, optimize spatial arrangements, and streamline the construction workflow. As CAD designs continue to grow in complexity, automating the detection and interpretation of symbols within these floorplans becomes increasingly important in various downstream tasks, such as code compliance checking and 3D interior modeling [20].

Despite the progress made in symbol recognition, the task of panoptic symbol spotting in CAD drawings remains under-explored. The challenges are multifaceted, arising from the vast diversity of symbol types, the need to differentiate between visually similar symbols, and the presence of overlapping elements. Additionally, variations in scale, orientation, and stylistic representation further complicate accurate identification.

Traditional methods approached symbol recognition in a query-by-example manner [29], but these techniques struggle to handle the vast diversity of graphical symbols in real-world datasets. More recent learning-based approaches [7, 25] have shown significant progress in addressing the symbol spotting task. Early solutions [5, 27, 39] typically leverage convolutional neural networks (CNNs) or graph-based models to spot symbols. More advanced methods leverage Transformer architectures and attention mechanisms [6, 39], improving global relationship reasoning among symbols. These methods use rasterized pixel images derived from vector CAD drawings as input. Such conversion, however, introduces discrepancies between the original vector graphics and the rasterized images, resulting in errors due to the loss of precise geometric information.

The representative work SymPoint [16] treats CAD drawings as sets of primary points, leveraging techniques from point cloud analysis for effective CAD symbol spotting. Such a representation simplifies model complexity while achieving strong performance on panoptic symbol spotting tasks in CAD drawings. Building on this foundation, SymPoint-V2 [17] introduces Layer feature-enhanced encoding to incorporate graphical layer information and a position-guided Training method to enhance model learning and accelerate convergence. Yet both approaches rely on manually defined primitive feature representations, i.e., four fixed primitive types. As a result, they struggle to capture the full diversity of CAD graphical primitives. In addition, these methods focus on processing small to medium-scale datasets due to the absence of efficient strategies for preserving connectivity during symbol spotting across expansive drawings. By far, there is still a lack of efficient methods to address the panoptic symbol spotting task in large-scale CAD drawings, as dense symbol clutter and significant variations in scale present substantial challenges for accurate segmentation and symbol recognition.

In this paper, we present CADSpotting, a simple yet highly effective panoptic symbol spotting method tailored

for handling CAD drawings at a much larger scale. Specifically, CADSpotting does not rely on fixed graphic primitive types. Instead, it densely samples points along CAD graphic primitives to construct comprehensive point cloud representations. Each point is represented by basic attributes, such as coordinates and color, forming a lightweight but expressive feature set. We utilize a unified 3D point cloud processing model to learn robust features from the sampled points. CADSpotting then employs a streamlined Transformer decoder module for panoptic symbol spotting, effectively leveraging the detailed learned features to achieve precise segmentation. To handle large-scale, real-world CAD drawings, we further propose a novel Sliding Window Aggregation (SWA) technique, combining a weighted voting strategy with Non-Maximum Suppression (NMS) to enable accurate and efficient panoptic segmentation.

On the data front, we further introduce LS-CAD, a new large-scale CAD dataset containing 50 annotated floorplans from a variety of building types, including campuses and office complexes. Each drawing follows the same fine-grained annotation standards as the FloorPlanCAD dataset, with an average coverage of over 1,000 square meters per floorplan. LS-CAD is the first dataset of its scale in this domain, part of which will be released to the research community under a license waiver, to stimulate further developments. Experimental results on both FloorPlanCAD and LS-CAD demonstrate that CADSpotting outperforms the state-of-the-art methods by a margin, demonstrating its robustness and effectiveness in handling the complexities of large-scale, real-world CAD drawings.

2. Related Work

Panoptic Image Segmentation. Image segmentation is a fundamental task in computer vision, traditionally divided into two main categories: semantic segmentation [1, 2, 18, 33, 35] and instance segmentation [8, 9, 13, 28]. Semantic segmentation assigns a class label to every pixel in an image, while instance segmentation distinguishes individual objects within the same class. Recently, SAM [13] introduces a large model trained on over one billion masks, leveraging prompt-based interactions for enhanced interactive segmentation. SAM2 [24] extends this approach to video segmentation. However, semantic and instance segmentation methods struggle to accurately represent uncountable background elements, such as the sky or terrain. To address this challenge, Kirillov et al. [12] propose Panoptic Segmentation, which unifies semantic and instance segmentation, effectively handling both countable and uncountable background components. Early approaches [3, 11, 15, 31] primarily employ CNN-based architectures, while recent advancements, such as Mask2Former [4], SegFormer [35], and OneFormer [9],

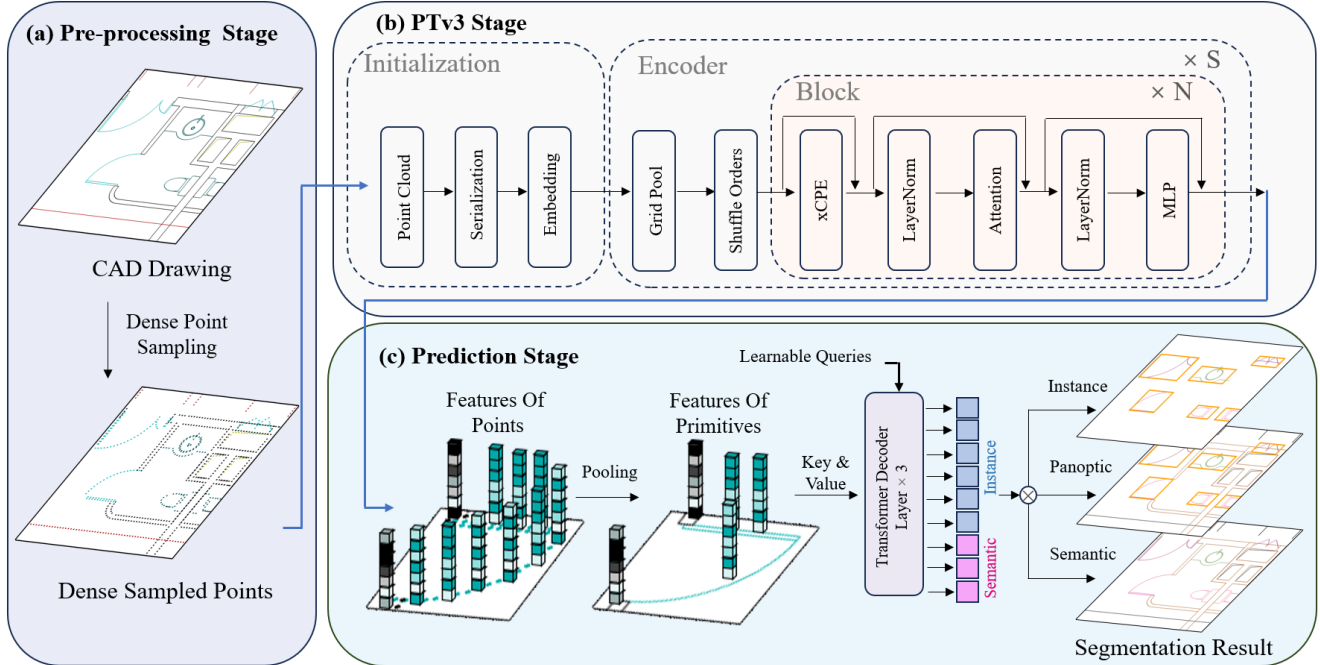


Figure 2. Overview of the CADSpotting method: Given a CAD drawing as input, CADSpotting first densely samples points along CAD graphic primitives to build a comprehensive point cloud representation, with each point defined by its coordinates and color. Next, Point Transformer V3 (PTv3) serves as the backbone, extracting robust features from the sampled points. We then apply mixed pooling to obtain the primitive-level features. Finally, a streamlined Transformer decoder is used for efficient panoptic symbol spotting.

leverage Transformer models, incorporating a mask attention mechanism to boost segmentation performance. Following the large-model paradigm of SAM, SEEM [40] further refines segmentation capabilities using a prompt-driven design. Despite these advances, most existing segmentation models remain pixel-centric, limiting their effectiveness in processing vector graphics like CAD drawings. Consequently, they often fail to capture critical vector-based information, such as overlapping relationships and precise geometric attributes.

CAD Symbol Spotting. Early efforts [10, 22, 23, 26, 36] in symbol spotting on CAD drawings rely on handcrafted feature descriptors, such as shape and structure, coupled with techniques like sliding window searches or graph matching for symbol retrieval. The introduction of deep learning techniques marked a significant shift, with models based on Faster R-CNN [25] and YOLO v3 [7] greatly enhancing the accuracy of symbol recognition tasks [27]. However, traditional symbol spotting methods are primarily designed for countable objects and do not effectively handle uncountable symbols, which are common in CAD environments. To address this limitation, Fan et al. [5] introduce the FloorPlanCAD dataset and CNN-GCN method, enabling the recognition of both countable and uncountable symbols for more comprehensive CAD parsing. Building on this, Zheng et al. [39] propose GAT-CADNet, a model

that represents CAD drawings as graph structures and performs segmentation by predicting adjacency matrices. Further advancements include CADTransformer [6], which utilizes the Vision Transformer to extract features from scalar maps, leading to improved predictions. Meanwhile, significant progress has been made in the field of 3D point cloud segmentation [14, 30, 34, 38]. The seminal work SymPoint [16] proposes a novel method that converts symbols into primary point representations, thereby enhancing feature extraction through point cloud analysis and upsampling techniques. Concurrently, Liu et al. [17] extend SymPoint by incorporating LFE and PGT modules, further improving feature representation and model performance. Despite these advances, the manually defined feature representation is often constrained by a limited set of graphical primitive types, which hinders their ability to capture the full diversity of CAD symbols.

3. Method

An overview of our CADSpotting method is provided in Fig. 2. By integrating a dense point sampling strategy within a unified point cloud processing model, our approach efficiently extracts features for CAD primitives, producing a robust representation that supports various primitive types. Details are provided in Sec. 3.1. Then, a straightforward transformer decoder is applied to perform semantic, in-

stance, and panoptic segmentation, with the corresponding loss function detailed in Sec.3.2. Additionally, we propose a novel Sliding Window Aggregation technique in Sec.3.3. Using a weighted voting strategy and Non-Maximum Suppression (NMS), this method allows our method to process expansive CAD drawings and perform large-scale panoptic segmentation.

3.1. Primitive Feature Learning

SymPoint [16] introduces a new concept that represents CAD primitives as a set of 2D points. It constructs a hand-crafted feature for each graphical primitive, capturing details such as type (e.g., line, arc, circle, ellipse), length, etc. SymPoint then applies point cloud analysis to learn primitive representations, further enhancing connectivity through an Attention with Connection Module. A masked-attention transformer decoder is used to complete the panoptic symbol spotting task. Although SymPoint demonstrates strong performance in CAD symbol spotting, its feature representation is manually defined and limited to four fixed primitive types, which may constrain its capacity to fully capture the diverse range of CAD symbols. To address these constraints, we propose a novel graphical primitive feature representation for CAD drawings that incorporates dense point sampling within a unified point cloud analysis model to improve both the efficiency and generalizability of primitive-level representations.

Dense Point Sampling. In CAD drawings, graphical primitives are typically categorized into line types and shape types. Line primitives encompass straight segments, curves, and complex contours such as Bézier curves, while shape primitives include basic geometric forms like rectangles, circles, and ellipses. Inspired by SymPoint [16], we propose a dense point sampling strategy that performs equidistant sampling on each primitive to generate dense point data for feature extraction. Rather than assigning fixed types to CAD graphical primitives and using hand-crafted features to represent them, our dense point sampling method offers greater efficiency and adaptability, making it suitable for a wide range of CAD primitives. Fig.3 illustrates the process of our dense point sampling method.

Given a CAD drawing containing N primitives, we perform dense sampling to generate a 2D point cloud P from these primitives at a fixed distance d . Each 2D point $p \in P$ is represented by a six-dimensional vector \mathbf{f} :

$$\mathbf{f} = (x, y, z, r, g, b) \in \mathbb{R}^6 \quad (1)$$

where x, y represent the 2D coordinates of the point, z is set to 0, and r, g, b represent the color information (red, green, blue channels) of the point. We then employ Point Transformer V3 [34] (PTv3) as the backbone for feature extraction, leveraging its design optimized for the unordered

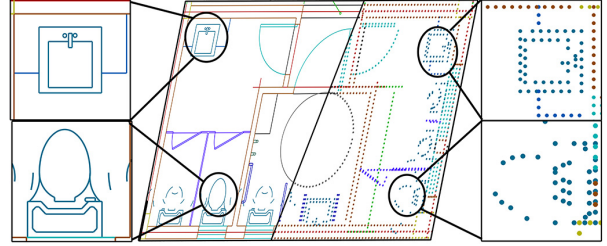


Figure 3. Dense point sampling. Left: A CAD drawing containing various primitives. Right: Dense point sampling converts each primitive symbol to a dense set of points.

nature of point clouds, which provides high efficiency and robust performance in feature extraction.

Feature Pooling. To obtain the final feature representation for CAD graphical primitives, we apply primitive mixed pooling to transform point-wise features into primitive-wise features. Specifically, we perform pooling on densely sampled points P within each primitive A , aggregating the point features of each primitive into a single primitive-wise feature vector:

$$\mathbf{f} \in \mathbb{R}^{M \times C} \rightarrow \mathbf{g} \in \mathbb{R}^{N \times C} \quad (2)$$

where M denotes the total number of 2D sampled points, and N represents the number of primitives. Let A_i represent a single primitive with its corresponding dense point cloud P_i . The c -th dimension feature of \mathbf{g}_i is determined by the sum of the maximum and average values of the corresponding c -th dimension features across all points P_i :

$$\mathbf{g}_i(c) = \max_{p \in P_i} \mathbf{f}_p(c) + \frac{1}{|P_i|} \sum_{p \in P_i} \mathbf{f}_p(c) \quad (3)$$

This pooling method condenses a large set of dense point features into a more compact set of primitive features, effectively reducing computational complexity and storage requirements. At the same time, primitive-wise pooling retains the essential information of the contained points, preserving global consistency in the primitive representation and minimizing information loss. Loss calculations are also conducted at the primitive level, aligning with our final goal of performing CAD spotting tasks.

3.2. Panoptic Symbol Spotting

We utilize a simple transformer decoder to extract semantic and instance symbol spotting information from the learned primitive features. In our model, the pooled primitive features serve as key and value inputs to three consecutive layers of Transformer decoders, where the self-attention mechanism effectively captures dependencies among the input features. The queries are initialized randomly and optimized during training to compute accurate self-attention scores with other features.

Following OneFormer3D [14], we partition the decoder output into two parts: the first K_{ins} outputs represent instance symbol spotting proposals, and the subsequent K_{sem} outputs correspond to semantic symbol spotting. This configuration enables panoptic symbol spotting by integrating instance and semantic information for comprehensive scene understanding. Here, K_{ins} is manually defined, and K_{sem} corresponds to the number of semantic categories.

We translate decoder outputs to semantic proposals and instance proposals. A semantic proposal includes the log-likelihood values for each primitive being classified into different semantic labels and can be further processed through thresholding to generate a binary mask. Similarly, an instance proposal also contains log-likelihood values, but these indicate the likelihood of each primitive being classified as a specific instance. During inference, we select the top- k instance proposals of the highest confidence scores and apply matrix-NMS [32] to suppress non-maximal instance predictions.

Loss Function. The loss function L is composed of classification loss and primitive mask loss. The classification loss L_{cls} is defined as a multi-class cross-entropy loss. The primitive mask loss combines binary cross-entropy loss, L_{bce} , with the Dice loss [21], L_{dice} , to evaluate the correspondence between each predicted instance and its ground truth counterpart.

$$L = \lambda_{\text{cls}}L_{\text{cls}} + \lambda_{\text{bce}}L_{\text{bce}} + \lambda_{\text{dice}}L_{\text{dice}} \quad (4)$$

3.3. Sliding Window Aggregation

To address the challenge of panoptic symbol segmentation at large scales, a key issue is ensuring the generalization of instance symbol segmentation across varying scales. During inference on larger drawings than those encountered during training, the network must produce significantly more instance proposals. However, this process is limited by the fixed number of instance queries inherent in Mask Transformer-based methods, a constraint that also affects our approach. Nonetheless, CAD instance symbol segmentation offers certain advantages over general image instance segmentation. Specifically, in CAD floorplans, instances of the same category maintain relatively consistent sizes across different scenes when a uniform scale is applied. Consequently, we can reasonably assume that the size of instances in inference will not exceed that of the same category in the training images.

Therefore, we propose using a fixed-size window based on the training image dimensions and apply 2D sliding window inference on the large input drawings. For each sliding window, once the primitives intersect with or are encompassed by the window, we utilize the features of these primitives along with the window’s semantic and instance

Building	Area(m^2)	#Primitive	#Instance
Office 1	3,912	3,910	406
Office 2	1,799	28,193	1,185
Office 3	2,994	16,803	559
Campus 1	1,949	12,571	603
Hotel 1	1,193	26,709	335

Table 1. Summary statistics for five samples from the LS-CAD Dataset.

proposals, thereby increasing the likelihood of fully capturing potential instances. After gathering proposals across all windows, we apply distinct aggregation strategies for semantic and instance proposals.

For semantic proposals, we use a voting scheme to predict each primitive’s semantic label, treating each primitive as an independent unit. Primitives that extend across larger spatial areas may be captured by multiple windows. In such cases, we prioritize proposals that capture the primitive as completely as possible by using weighted voting, where each window’s voting weight is determined by the proportion of the primitive’s dense points observed relative to the total dense points of that primitive.

For instance proposals, we directly apply Non-Maximum Suppression (NMS) to the instance proposals obtained from all windows. A potential instance may be partially or fully observed across multiple windows. By ensuring a sufficiently small sliding step size, each instance is fully captured within at least one window. Incomplete proposals from other windows are subsequently filtered out during the NMS process.

4. Experiments

4.1. LS-CAD Dataset

We introduce LS-CAD, a new large-scale CAD dataset consisting of 50 floorplans from extensive buildings, such as campuses and office buildings. Each CAD drawing in LS-CAD covers an area of at least 1,000 square meters, with the number of primitives ranging from approximately 2,900 to over ten thousand. Table.1 showcases five large-scale CAD drawings from our dataset, providing detailed information such as area, number of primitives and instance count, which underscore the large-scale nature of LS-CAD.

Additionally, the floorplans in LS-CAD include a wide variety of complex symbols, such as doors, windows, walls, stairs, elevators, different types of furniture, and parking spaces. We provide fine-grained annotations consistent with the standards of the FloorPlanCAD [5] dataset. A portion of LS-CAD will be publicly available under a license waiver to support further research in panoptic symbol spotting for large-scale CAD drawings.

Methods	F1	wF1	mIoU
PanCADNet [5]	80.6	79.8	-
CADTransformer [6]	82.2	90.1	-
GAT-CADNet [39]	85.0	82.3	-
SymPoint [16]	86.8	85.5	69.7
SymPoint-V2 [17]	89.5	88.3	74.7
CADSpotting (ours)	93.5	93.9	83.3

Table 2. Quantitative comparison of semantic symbol spotting.

Methods	AP50	AP75	mAP
DINO [37]	64.0	54.9	47.5
SymPoint [16]	66.3	55.7	52.8
SymPoint-V2 [17]	71.3	60.7	60.1
CADSpotting (ours)	72.2	69.1	69.0

Table 3. Quantitative comparison of instance symbol spotting.

4.2. Experimental Settings

Implementation Details. We use the train split of the FloorPlanCAD dataset to train our model. The FloorPlanCAD dataset comprises approximately 15,000 drawings, annotated across 35 symbol categories, including 30 things and 5 stuff classes. For dense point sampling, we set a fixed distance $d = 0.14$. Model training is performed on a machine with 8 NVIDIA A100 GPUs, using a batch size of 2 per GPU for 512 epochs. We use the AdamW [19] optimizer with a learning rate of 10^{-4} and a weight decay of 0.05. Data augmentation techniques include random horizontal flipping with a probability of 0.5, global rotation and scaling transformations, translation along the x and y axes and color normalization to $[-1, 1]$. We set loss weight as $\lambda_{cls} : \lambda_{bce} : \lambda_{dice} = 0.5 : 1 : 1$. Additionally, we set $K_{sem} = 36$ as the number of semantic labels, and both the top- k value and K_{ins} are set to 220. We use $\Delta = 70$ as the step size of Sliding Window Aggregation on LS-CAD dataset.

Metrics. Following the approach of [6], we assess the performance of our model using multiple metrics. For semantic symbol spotting, we use F1 score, weighted F1 score (wF1), and mean Intersection over Union (mIoU). For instance symbol spotting, we employ AP50, AP75, and mean Average Precision (mAP). For panoptic symbol spotting, we utilize Panoptic Quality (PQ), Segmentation Quality (SQ), and Recognition Quality (RQ). PQ, in particular, is a comprehensive metric combining SQ and RQ to evaluate model performance in semantic and instance segmentation tasks. Further details on metric formulation are available in [6].

4.3. Quantitative Evaluation

To demonstrate the effectiveness of our approach, we compare it against SOTA and concurrent methods on the FloorPlanCAD [5] and LS-CAD datasets. A detailed comparison

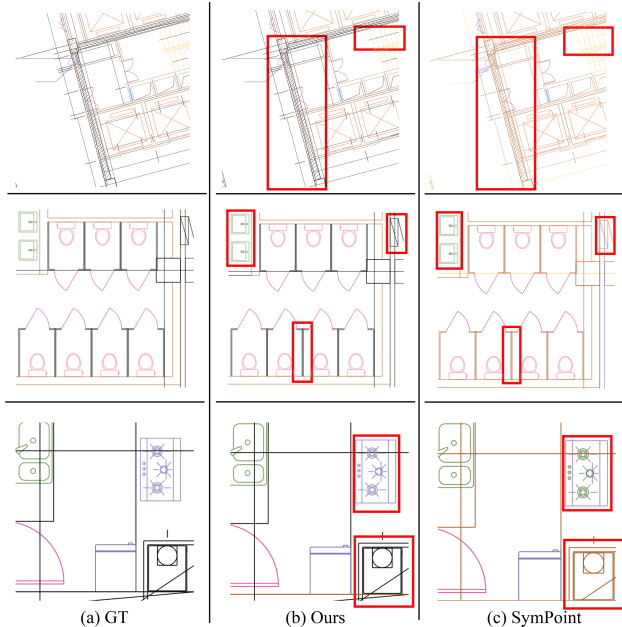


Figure 4. Qualitative comparison of semantic symbol spotting. Our dense point sampling based primitive feature learning enables our approach to achieve precise semantic segmentation, particularly on walls and complex, overlapping symbols such as faucets in sinks and uncommon furniture symbols.

of semantic, instance, and panoptic symbol spotting tasks is provided in the following paragraphs.

Semantic Symbol Spotting. As shown in Table.2, we compare our method with PanCADNet [5], CADTransformer [6], GAT-CADNet [39], SymPoint [16] and the concurrent SymPoint-V2 [17]. Our CADSpotting approach achieves the highest performance in both the F1 and wF1 metrics, outperforming SymPoint by 13.6% and SymPoint-V2 by 8.6% in mIoU.

Instance Symbol Spotting. We also evaluate our method against DINO [37], SymPoint and SymPoint-V2 for instance symbol spotting, using the bounding box maximization of predicted mask to compute the AP metric, consistent with SymPoint. As illustrated in Table.3, our method achieves superior results in the AP50, AP75 and mAP metrics, with improvements of 0.9% AP50, 8.4% AP75 and 8.9% mAP over SymPoint-V2.

Panoptic Symbol Spotting. We then compare our method with the same SOTA and concurrent methods used in the semantic symbol spotting comparison. The results, presented in Table.4, show that our approach surpasses SymPoint and other prior methods across all metrics, including Total/Thing/Stuff PQ, SQ and RQ. Our method

Method	Total			Thing			Stuff		
	PQ	SQ	RQ	PQ	SQ	RQ	PQ	SQ	RQ
PanCADNet [5]	59.5	82.6	66.9	65.6	86.1	76.1	58.7	81.3	72.2
CADTransformer [6]	68.9	88.3	73.3	78.5	94.0	83.5	58.6	81.9	71.5
GAT-CADNet [39]	73.7	91.4	80.7	-	-	-	-	-	-
SymPoint [16]	83.3	91.4	91.1	84.1	94.7	88.8	48.2	69.5	69.4
SymPoint-V2 [17]	90.1	96.3	93.6	90.8	96.6	94.0	80.8	90.9	88.9
CADSpotting (Ours)	88.9	95.6	93.0	89.7	96.2	93.2	80.6	89.7	89.8

Table 4. Quantitative comparison of panoptic symbol spotting. Orange and blue cell colors indicate the best and the second-best results. Our method achieves slightly worse performance than a concurrent work SymPoint-V2, but it excels in scalability and robustness, as demonstrated in large-scale CAD drawings with diverse symbol primitives.

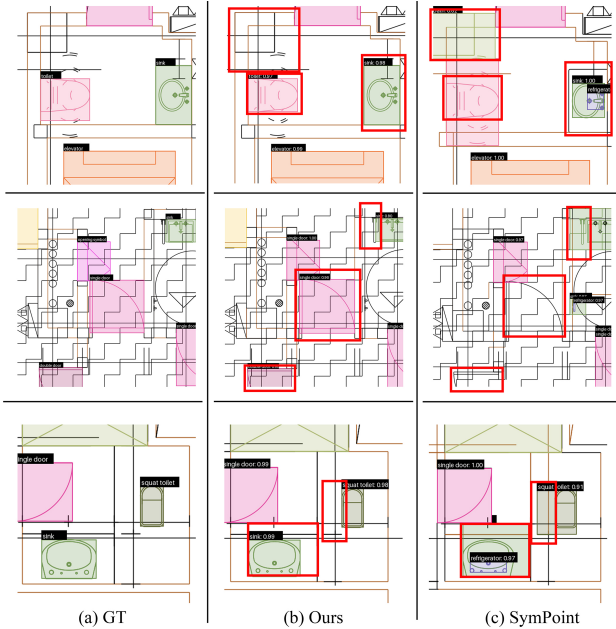


Figure 5. Qualitative comparison of panoptic symbol spotting. Our method accurately detects symbol instances, even in situations where symbols are overlapped by other elements.

achieves results comparable to the concurrent SymPoint-V2, with only a slight performance gap of no more than 1.2% , except for RQ in the Stuff type, where our method outperforms. Additionally, our approach offers superior generalization across diverse CAD primitives, thanks to its dense point sampling based feature representation.

We also compare CADSpotting with SymPoint on our LS-CAD dataset. Since the original SymPoint cannot directly process large-scale CAD drawings, we first apply straightforward block partitioning, using the same size as drawings the FloorPlanCAD dataset without overlapping between blocks, to divide large-scale CAD drawings into smaller blocks for input into SymPoint, referred to as SymPointBP. The results in Table.7 show that our method with block partitioning (CADSpottingBP) achieves the highest performance in SQ. Our method with the SWA technique

Primitive Pooling Type	PQ	SQ	RQ
w/o Pooling	74.6	89.3	83.6
Max	86.1	94.1	91.5
Average	87.6	94.5	92.7
Mixed (Max+Average)	88.9	95.6	93.0

Table 5. Ablation study on different pooling methods.

(CADSpottingSWA) achieves results comparable to SymPointBP and CADSpottingBP, with an absolute improvement of 2.5% in SQ compared to SymPointBP and a slight decrease of 0.8% compared to CADSpottingBP. However, CADSpottingSWA significantly outperforms SymPointBP in PQ and RQ, with an improvement of at least 20%, demonstrating that our CADSpotting method with the SWA technique can accurately recognize instances of CAD symbols in large-scale CAD drawings.

4.4. Qualitative Comparison

We perform qualitative comparisons with SymPoint on the FloorPlanCAD dataset. Fig.4 and Fig.5 show that our method achieves accurate and robust semantic and panoptic symbol spotting, even in challenging scenarios involving walls, complex or overlapping symbols, and uncommon furniture symbols. This demonstrates the effectiveness of our proposed dense point sampling based primitive features. Additionally, Fig.6 presents our semantic and panoptic symbol spotting results on a large-scale CAD drawing of an office building with 28,193 primitives and 1,185 instances from our LS-CAD dataset. These results demonstrate that our CADSpotting enhanced by SWA technique, accurately identifies semantic and instance information in large-scale CAD drawings.

4.5. Ablation Studies

Feature Learning. We compare our dense point sampling based primitive feature learning method with the approach in SymPoint, which uses handcrafted features to represent each individual primitive. SymPoint employs Point Transformer(PTv1) [38] as its backbone network and incorporates hierarchical multi-resolution primitive features to

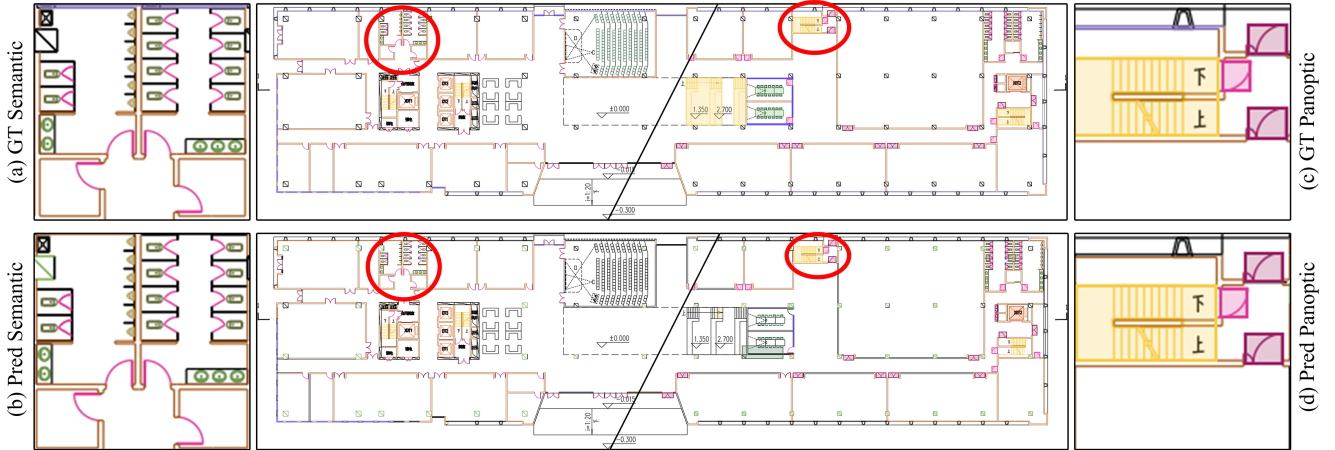


Figure 6. Semantic and panoptic symbol spotting results of CADSpotting with the SWA technique on a large-scale office building CAD drawing from our LS-CAD dataset. The figure shows full CAD drawings with GT and predicted results in the center, with closeup views of GT in (a, c) and predicted results in (b, d).

Methods	Backbone	PQ	SQ	RQ
Handcrafted Features	PTv1	78.4	88.5	88.6
Handcrafted Features	PTv3	80.2	90.2	89.0
Ours	PTv3	88.9	95.6	93.0

Table 6. Ablation study on feature learning methods. We compare our dense point sampling based primitive features with the handcrafted feature representations in SymPoint. All methods utilize the same decoder architecture to learn intermediate features.

Method	PQ	SQ	RQ
SymPoint + Block Partitioning	33.5	84.6	39.6
Ours + Block Partitioning	50.1	87.9	56.6
Ours + SWA	54.3	87.1	61.8

Table 7. Quantitative comparison of semantic and panoptic symbol spotting on LS-CAD dataset.

leverage intermediate features, enhancing the decoder’s performance. To evaluate the impact of different point cloud analysis methods, we first replace SymPoint’s backbone with PTv3 [34], maintaining the same decoder architecture as ours to ensure a fair comparison of feature learning techniques in panoptic symbol spotting. As shown in Table.6, with the same decoder configuration, simply switching to PTv3 results in a 1.8% improvement in PQ. When we apply our proposed primitive feature learning method, performance further increases by 8.7% in PQ, demonstrating the significant performance gains achieved by our dense point sampling based feature learning approach.

Pooling. We further evaluate the necessity and impact of different pooling methods on our approach, using a baseline configuration without a pooling layer. As shown in Table 5, max pooling improves performance by 11.5%, average pooling by 13.0%, and mixed pooling by 14.3% in

PQ. Based on these results, we select mixed pooling for our CADSpotting approach.

Partitioning. Table.7 shows that our method with the SWA technique (CADSpottingSWA) yields results comparable to our method using block partitioning (CADSpottingBP), with only a slight decrease of 0.8% in SQ. However, CADSpottingSWA surpasses CADSpottingBP in PQ and RQ by a margin, highlighting the effectiveness of the Sliding Window Aggregation technique in panoptic symbol spotting for large-scale CAD drawings.

5. Conclusion

We have introduced CADSpotting, a novel approach for panoptic symbol spotting in large-scale CAD drawings. Our method utilizes dense point sampling within a unified point cloud processing framework to effectively learn robust feature representations of CAD primitives. To address the challenges of precise segmentation in complex, large-scale floorplans, we propose a Sliding Window Aggregation technique, which combines weighted voting with Non-Maximum Suppression to achieve precise symbol detection and segmentation. Additionally, we present LS-CAD, a new large-scale dataset containing 50 annotated CAD floorplans from diverse building types, providing a valuable benchmark for the CAD symbol spotting task. Experimental results on both the LS-CAD and FloorPlanCAD datasets demonstrate the effectiveness, scalability, and robustness of our approach.

Despite these advancements, one limitation of our method is its panoptic symbol spotting performance on large-scale CAD drawings, which currently lags behind its performance on smaller-scale datasets like FloorPlanCAD. Addressing this gap is a focus of our ongoing and future

work. We also plan to extend our approach to joint symbol spotting and 3D model generation across multiple building layers, moving towards the goal of fully automated 3D building reconstruction from CAD drawings.

References

- [1] Liang-Chieh Chen. Rethinking atrous convolution for semantic image segmentation. *arXiv preprint arXiv:1706.05587*, 2017. 2
- [2] Liang-Chieh Chen, George Papandreou, Iasonas Kokkinos, Kevin Murphy, and Alan L Yuille. Deeplab: Semantic image segmentation with deep convolutional nets, atrous convolution, and fully connected crfs. *IEEE transactions on pattern analysis and machine intelligence*, 40(4):834–848, 2017. 2
- [3] Liang-Chieh Chen, Huiyu Wang, and Siyuan Qiao. Scaling wide residual networks for panoptic segmentation. *arXiv preprint arXiv:2011.11675*, 2020. 2
- [4] Bowen Cheng, Ishan Misra, Alexander G Schwing, Alexander Kirillov, and Rohit Girdhar. Masked-attention mask transformer for universal image segmentation. In *Proceedings of the IEEE/CVF conference on computer vision and pattern recognition*, pages 1290–1299, 2022. 2
- [5] Zhiwen Fan, Lingjie Zhu, Honghua Li, Xiaohao Chen, Siyu Zhu, and Ping Tan. Floorplancad: A large-scale cad drawing dataset for panoptic. In *Proceedings of the IEEE/CVF international conference on computer vision*, pages 10128–10137, 2021. 2, 3, 5, 6, 7
- [6] Zhiwen Fan, Tianlong Chen, Peihao Wang, and Zhangyang Wang. Cadtransformer: Panoptic symbol spotting transformer for cad drawings. In *Proceedings of the IEEE/CVF Conference on Computer Vision and Pattern Recognition*, pages 10986–10996, 2022. 2, 3, 6, 7
- [7] Ali Farhadi and Joseph Redmon. Yolov3: An incremental improvement. In *Computer vision and pattern recognition*, pages 1–6. Springer Berlin/Heidelberg, Germany, 2018. 2, 3
- [8] Kaiming He, Georgia Gkioxari, Piotr Dollár, and Ross Girshick. Mask r-cnn. In *Proceedings of the IEEE international conference on computer vision*, pages 2961–2969, 2017. 2
- [9] Jitesh Jain, Jiachen Li, Mang Tik Chiu, Ali Hassani, Nikita Orlov, and Humphrey Shi. Oneformer: One transformer to rule universal image segmentation. In *Proceedings of the IEEE/CVF Conference on Computer Vision and Pattern Recognition*, pages 2989–2998, 2023. 2
- [10] Xinyang Jiang, Lu Liu, Caihua Shan, Yifei Shen, Xuanyi Dong, and Dongsheng Li. Recognizing vector graphics without rasterization. *Advances in Neural Information Processing Systems*, 34:24569–24580, 2021. 3
- [11] Alexander Kirillov, Ross Girshick, Kaiming He, and Piotr Dollár. Panoptic feature pyramid networks. In *Proceedings of the IEEE/CVF conference on computer vision and pattern recognition*, pages 6399–6408, 2019. 2
- [12] Alexander Kirillov, Kaiming He, Ross Girshick, Carsten Rother, and Piotr Dollár. Panoptic segmentation. In *Proceedings of the IEEE/CVF conference on computer vision and pattern recognition*, pages 9404–9413, 2019. 2
- [13] Alexander Kirillov, Eric Mintun, Nikhila Ravi, Hanzi Mao, Chloe Rolland, Laura Gustafson, Tete Xiao, Spencer Whitehead, Alexander C Berg, Wan-Yen Lo, et al. Segment anything. In *Proceedings of the IEEE/CVF International Conference on Computer Vision*, pages 4015–4026, 2023. 2
- [14] Maxim Kolodiaznyi, Anna Vorontsova, Anton Konushin, and Danila Rukhovich. Oneformer3d: One transformer for unified point cloud segmentation. In *Proceedings of the IEEE/CVF Conference on Computer Vision and Pattern Recognition*, pages 20943–20953, 2024. 3, 5
- [15] Yanwei Li, Xinze Chen, Zheng Zhu, Lingxi Xie, Guan Huang, Dalong Du, and Xingang Wang. Attention-guided unified network for panoptic segmentation. In *Proceedings of the IEEE/CVF conference on computer vision and pattern recognition*, pages 7026–7035, 2019. 2
- [16] WENLONG LIU, Tianyu Yang, Yuhan Wang, Qizhi Yu, and Lei Zhang. Symbol as points: Panoptic symbol spotting via point-based representation. In *The Twelfth International Conference on Learning Representations*, 2024. 2, 3, 4, 6, 7
- [17] Wenlong Liu, Tianyu Yang, Qizhi Yu, and Lei Zhang. Sympoint revolutionized: Boosting panoptic symbol spotting with layer feature enhancement. *arXiv preprint arXiv:2407.01928*, 2024. 2, 3, 6, 7
- [18] Jonathan Long, Evan Shelhamer, and Trevor Darrell. Fully convolutional networks for semantic segmentation. In *Proceedings of the IEEE conference on computer vision and pattern recognition*, pages 3431–3440, 2015. 2
- [19] I Loshchilov. Decoupled weight decay regularization. *arXiv preprint arXiv:1711.05101*, 2017. 6
- [20] MarsBIM. Cad to bim conversion. <https://www.marsbim.com/services/bim/cad-to-bim-conversion/>. Accessed: 2024-11-10. 2
- [21] Fausto Milletari, Nassir Navab, and Seyed-Ahmad Ahmadi. V-net: Fully convolutional neural networks for volumetric medical image segmentation. In *2016 fourth international conference on 3D vision (3DV)*, pages 565–571. Ieee, 2016. 5
- [22] Thi-Oanh Nguyen, Salvatore Tabbone, and O Ramos Terrades. Symbol descriptor based on shape context and vector model of information retrieval. In *2008 The Eighth IAPR International Workshop on Document Analysis Systems*, pages 191–197. IEEE, 2008. 3
- [23] Thi-Oanh Nguyen, Salvatore Tabbone, and Alain Boucher. A symbol spotting approach based on the vector model and a visual vocabulary. In *2009 10th International Conference on Document Analysis and Recognition*, pages 708–712. IEEE, 2009. 3
- [24] Nikhila Ravi, Valentin Gabeur, Yuan-Ting Hu, Ronghang Hu, Chaitanya Ryali, Tengyu Ma, Haitham Khedr, Roman Rädle, Chloe Rolland, Laura Gustafson, et al. Sam 2: Segment anything in images and videos. *arXiv preprint arXiv:2408.00714*, 2024. 2
- [25] Shaoqing Ren, Kaiming He, Ross Girshick, and Jian Sun. Faster r-cnn: Towards real-time object detection with region proposal networks. *IEEE transactions on pattern analysis and machine intelligence*, 39(6):1137–1149, 2016. 2, 3

- [26] Alireza Rezvaniyar, Melissa Cote, and Alexandra Branzan Albu. Symbol spotting for architectural drawings: state-of-the-art and new industry-driven developments. *IPSI Transactions on Computer Vision and Applications*, 11:1–22, 2019. 3
- [27] Alireza Rezvaniyar, Melissa Cote, and Alexandra Branzan Albu. Symbol spotting on digital architectural floor plans using a deep learning-based framework. *2020 IEEE/CVF Conference on Computer Vision and Pattern Recognition Workshops (CVPRW)*, pages 2419–2428, 2020. 2, 3
- [28] Olaf Ronneberger, Philipp Fischer, and Thomas Brox. U-net: Convolutional networks for biomedical image segmentation. In *Medical image computing and computer-assisted intervention—MICCAI 2015: 18th international conference, Munich, Germany, October 5-9, 2015, proceedings, part III 18*, pages 234–241. Springer, 2015. 2
- [29] Maçal Rusiñol, Josep Lladós, and Gemma Sánchez. Symbol spotting in vectorized technical drawings through a lookup table of region strings. *Pattern Analysis and Applications*, 13:321–331, 2010. 2
- [30] Jonas Schult, Francis Engelmann, Alexander Hermans, Or Litany, Siyu Tang, and Bastian Leibe. Mask3d: Mask transformer for 3d semantic instance segmentation. In *2023 IEEE International Conference on Robotics and Automation (ICRA)*, pages 8216–8223. IEEE, 2023. 3
- [31] Ke Sun, Yang Zhao, Borui Jiang, Tianheng Cheng, Bin Xiao, Dong Liu, Yadong Mu, Xinggang Wang, Wenyu Liu, and Jingdong Wang. High-resolution representations for labeling pixels and regions. *arXiv preprint arXiv:1904.04514*, 2019. 2
- [32] Xinlong Wang, Rufeng Zhang, Tao Kong, Lei Li, and Chunhua Shen. Solov2: Dynamic and fast instance segmentation. *Advances in Neural Information Processing Systems*, 33:17721–17732, 2020. 5, 1
- [33] Huikai Wu, Junge Zhang, Kaiqi Huang, Kongming Liang, and Yizhou Yu. Fastfcn: Rethinking dilated convolution in the backbone for semantic segmentation. *arXiv preprint arXiv:1903.11816*, 2019. 2
- [34] Xiaoyang Wu, Li Jiang, Peng-Shuai Wang, Zhijian Liu, Xihui Liu, Yu Qiao, Wanli Ouyang, Tong He, and Hengshuang Zhao. Point transformer v3: Simpler faster stronger. In *Proceedings of the IEEE/CVF Conference on Computer Vision and Pattern Recognition*, pages 4840–4851, 2024. 3, 4, 8
- [35] Enze Xie, Wenhai Wang, Zhiding Yu, Anima Anandkumar, Jose M Alvarez, and Ping Luo. Segformer: Simple and efficient design for semantic segmentation with transformers. *Advances in neural information processing systems*, 34:12077–12090, 2021. 2
- [36] Bingchen Yang, Haiyong Jiang, Hao Pan, and Jun Xiao. Vectorfloorseg: Two-stream graph attention network for vectorized roughcast floorplan segmentation. In *Proceedings of the IEEE/CVF Conference on Computer Vision and Pattern Recognition*, pages 1358–1367, 2023. 3
- [37] Hao Zhang, Feng Li, Shilong Liu, Lei Zhang, Hang Su, Jun Zhu, Lionel Ni, and Heung-Yeung Shum. Dino: Detr with improved denoising anchor boxes for end-to-end object detection. In *The Eleventh International Conference on Learning Representations*, 2022. 6
- [38] Hengshuang Zhao, Li Jiang, Jiaya Jia, Philip HS Torr, and Vladlen Koltun. Point transformer. In *Proceedings of the IEEE/CVF international conference on computer vision*, pages 16259–16268, 2021. 3, 7
- [39] Zhaohua Zheng, Jianfang Li, Lingjie Zhu, Honghua Li, Frank Petzold, and Ping Tan. Gat-cadnet: Graph attention network for panoptic symbol spotting in cad drawings. In *Proceedings of the IEEE/CVF conference on computer vision and pattern recognition*, pages 11747–11756, 2022. 2, 3, 6, 7
- [40] Xueyan Zou, Jianwei Yang, Hao Zhang, Feng Li, Linjie Li, Jianfeng Wang, Lijuan Wang, Jianfeng Gao, and Yong Jae Lee. Segment everything everywhere all at once. *Advances in Neural Information Processing Systems*, 36, 2024. 3

CADSpotting: Robust Panoptic Symbol Spotting on Large-Scale CAD Drawings

Supplementary Material

A. LS-CAD Dataset

In Figure 8, we present visualizations of several samples from the LS-CAD dataset to highlight the diversity of the proposed dataset. The top panel illustrates Office 3, as described in the main text, which spans a floor area of $2,994m^2$ and includes 16,803 primitives and 559 instances. The bottom panel depicts Hotel 1, also described in the main text, which spans a floor area of $1,193m^2$ and includes 26,709 primitives and 335 instances.

B. Quantitative Evaluation

Detailed Ablation Study Results We present a comprehensive evaluation of panoptic quality (PQ), segmentation quality (SQ), and recognition quality (RQ) for each class, comparing different feature learning methods. Our final approach achieves superior performance across the majority of classes, particularly excelling in commonly used categories such as door classes, window classes, and wall classes. The detailed results are shown in Table 9.

C. Qualitative Evaluation

We provide visual comparisons of prediction results on different datasets. For FloorplanCAD, we compare the ground truth (GT) and predicted results using their primitive colors to intuitively evaluate prediction accuracy, as shown in Figure 9 and 10. For LS-CAD, we present the results of semantic and panoptic predictions, highlighting the performance of the method in practical scenarios, as shown in Figure 11 and 12.

D. Inference Time

We conducted a test and comparison of inference speeds for different methods on the FloorplanCAD test set using a single A6000 GPU. The results are presented in Table 8.

Method	Backbone	Pooling	Speed
Handcrafted Features	PTv1	×	83ms
Handcrafted Features	PTv3	×	60ms
Ours	PTv3	×	133ms
Ours	PTv3	✓	90ms

Table 8. Inference speeds of different methods on a single SVG file using an NVIDIA A6000 GPU. The **Ours** method is based on dense point sampling.

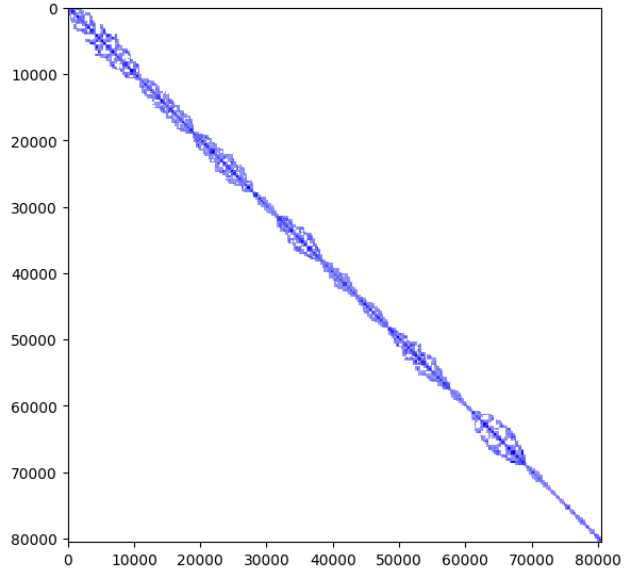
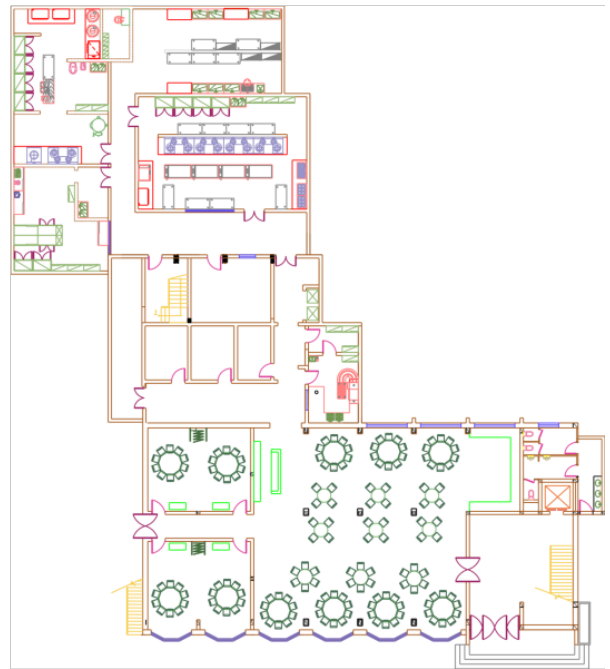
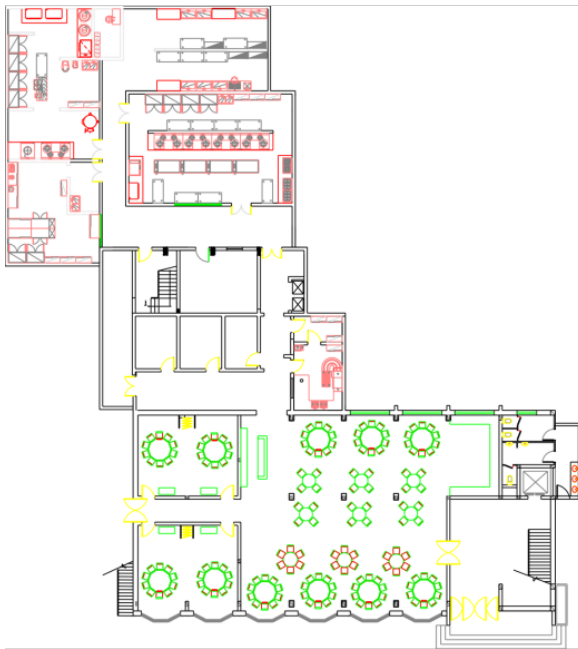
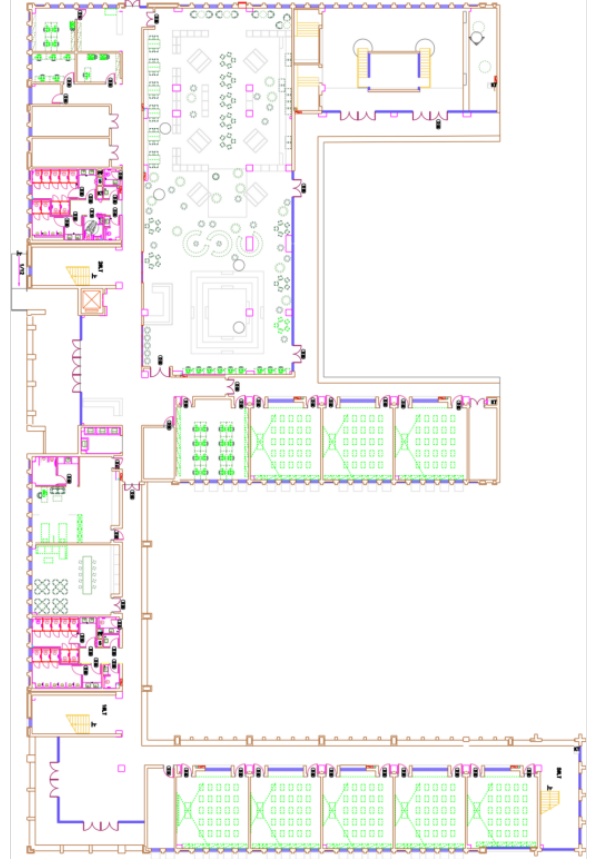
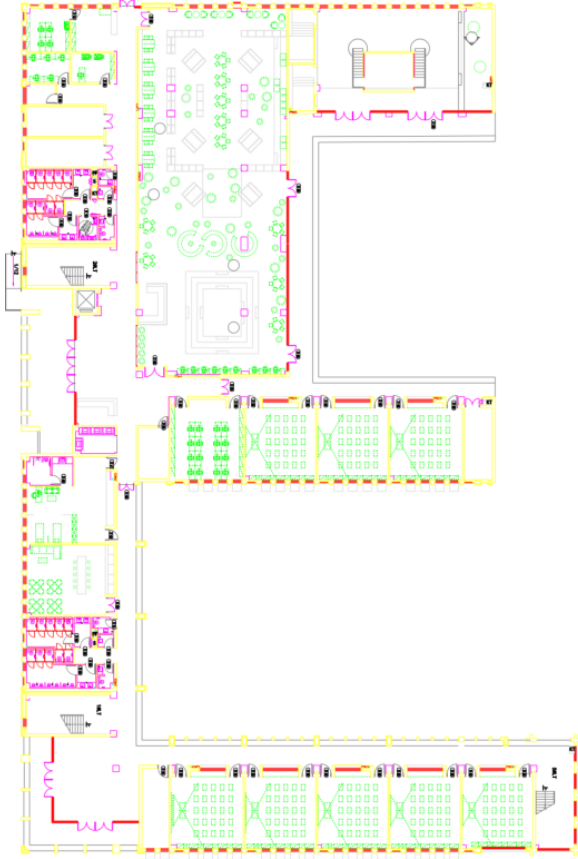


Figure 7. Visualization of the sparsity structure of the IoU matrix during sliding window aggregation for a sample drawing from the LS-CAD dataset. The Reverse Cuthill-McKee (RCM) algorithm was applied to reorder the matrix rows and columns, reducing its bandwidth and improving the visualization.

E. Sliding Window Implementation Details

In the matrix-NMS [32] process for sliding window aggregation, computing the Intersection over Union (IoU) between all pairs of instance proposal masks is essential for constructing the IoU matrix. However, the number of instance proposals grows substantially with the size of the input drawing. If a dense matrix representation is used, both the time and memory complexities of this operation become prohibitively high.

To mitigate this issue, we observe that only a small fraction of proposal pairs exhibit nonzero overlap, as most proposals belong to different inference windows. Figure 7 visualizes the sparsity structure of the IoU matrix during sliding window aggregation. By leveraging this sparsity, we reimplemented the IoU computation using sparse matrix routines, significantly reducing computational cost and memory usage without sacrificing accuracy.



(a) Raw Input

(b) GT

Figure 8. Examples from the LS-CAD Dataset. The figure shows the raw input and ground truth of two samples in the dataset. The raw input represents the unprocessed original svg image, while the ground truth is the svg image generated based on manually annotated labels, which facilitates the visualization and comparison of results. This dataset is designed to assess the performance of CAD image processing algorithms.

class	A			B			C			D		
	PQ	SQ	RQ	PQ	SQ	RQ	PQ	SQ	RQ	PQ	SQ	RQ
single door	91.59	97.08	94.34	75.67	90.68	83.44	87.23	92.68	94.12	87.46	92.85	94.20
double door	93.51	96.93	96.47	75.14	88.76	84.65	87.30	91.85	95.04	88.27	92.73	95.18
sliding door	96.54	98.78	97.73	83.55	50.31	83.55	94.51	96.15	98.29	91.32	95.65	95.46
folding door	57.67	87.88	65.62	39.66	95.83	41.38	70.88	83.29	85.11	52.03	82.64	62.96
revolving door	0.00	0.00	0.00	0.00	0.00	0.00	0.00	0.00	0.00	0.00	0.00	0.00
rolling door	0.00	0.00	0.00	0.00	0.00	0.00	0.00	0.00	0.00	0.00	0.00	0.00
window	89.60	97.24	92.14	75.49	91.87	82.17	77.13	85.24	90.49	74.53	85.06	87.62
bay window	48.15	95.26	50.55	41.92	88.51	47.37	22.25	77.38	28.75	12.00	68.83	17.44
blind window	90.57	98.17	92.25	77.71	96.14	80.83	79.56	84.85	93.76	77.28	83.91	92.10
opening symbol	46.64	76.82	60.71	37.97	72.60	52.30	36.47	79.11	46.10	20.10	72.22	27.84
sofa	88.53	96.29	91.93	71.82	82.05	87.53	76.98	90.28	85.28	73.74	87.40	84.37
bed	89.79	92.47	97.11	78.30	83.76	93.47	76.87	86.26	89.11	76.51	84.44	90.61
chair	83.58	94.04	88.88	70.05	85.54	81.89	84.42	92.26	91.51	80.85	91.71	88.16
table	75.39	88.46	85.22	53.18	78.36	67.87	68.03	86.46	78.68	61.99	86.43	71.72
TV cabinet	95.23	97.57	97.60	82.85	86.79	95.46	89.99	93.41	96.33	79.94	85.50	93.49
Wardrobe	93.76	97.23	96.43	84.53	89.58	94.36	85.37	88.77	96.17	82.50	85.94	95.99
cabinet	81.40	91.16	89.28	65.83	81.45	80.82	71.37	82.66	86.33	69.15	83.42	82.90
gas stove	97.34	99.17	98.16	90.08	96.15	93.69	97.10	97.89	99.19	96.66	97.61	99.03
sink	87.59	95.21	92.00	76.13	91.10	83.57	84.88	90.98	93.30	83.42	90.03	92.65
refrigerator	91.96	96.24	95.55	71.86	81.87	87.78	81.70	87.44	93.44	80.28	85.58	93.80
air conditioner	86.53	99.02	87.39	78.66	96.36	81.64	80.59	92.04	87.56	75.45	91.70	82.27
bath	79.30	93.31	84.98	63.84	83.21	76.73	66.62	79.71	83.58	62.06	77.36	80.22
bath tub	85.00	91.92	92.47	70.96	82.90	85.61	69.94	80.14	87.27	64.82	78.13	82.96
washing machine	89.17	97.74	91.23	78.29	90.75	86.27	86.40	91.21	94.73	77.97	85.26	91.45
squat toilet	95.35	98.25	97.05	78.70	94.34	83.42	92.58	94.79	97.67	89.99	92.68	97.09
urinal	94.32	98.76	95.51	80.33	92.08	87.24	91.80	94.84	96.79	91.31	94.79	96.32
toilet	95.21	98.08	97.07	81.39	91.92	88.55	90.81	93.01	97.63	90.48	93.53	96.74
stairs	86.47	94.28	91.72	74.68	89.68	83.27	68.56	82.02	83.59	65.50	79.52	82.36
elevator	96.15	97.53	98.58	79.08	94.76	83.44	84.44	90.52	93.28	80.64	88.59	91.03
escalator	73.73	88.37	83.44	67.98	79.15	85.88	29.80	72.72	40.98	44.64	73.70	60.56
row chairs	85.16	94.94	89.71	82.45	92.43	89.21	85.69	94.53	90.65	84.45	93.99	89.86
parking spot	89.68	95.20	94.20	84.34	92.67	91.01	72.22	80.84	89.34	72.64	82.77	87.76
wall	82.37	88.83	92.73	75.08	81.61	66.81	81.86	65.29	68.74	44.48	65.44	67.97
curtain wall	64.80	89.88	72.09	64.17	84.45	75.98	60.25	87.36	73.90	37.62	73.21	51.39
railing	75.67	92.22	82.06	62.87	85.69	73.37	37.82	76.42	49.49	28.53	70.73	40.34
total	88.91	95.65	92.96	74.59	89.26	83.56	80.24	90.17	88.98	78.36	88.59	88.46

Table 9. Quantitative results of the ablation study for panoptic symbol spotting across different classes.

A: Dense point sampling + PTv3 + Pooling(Ours). B: Dense point sampling + PTv3. C: Handcrafted features + PTv3. D: Handcrafted features + PTv1

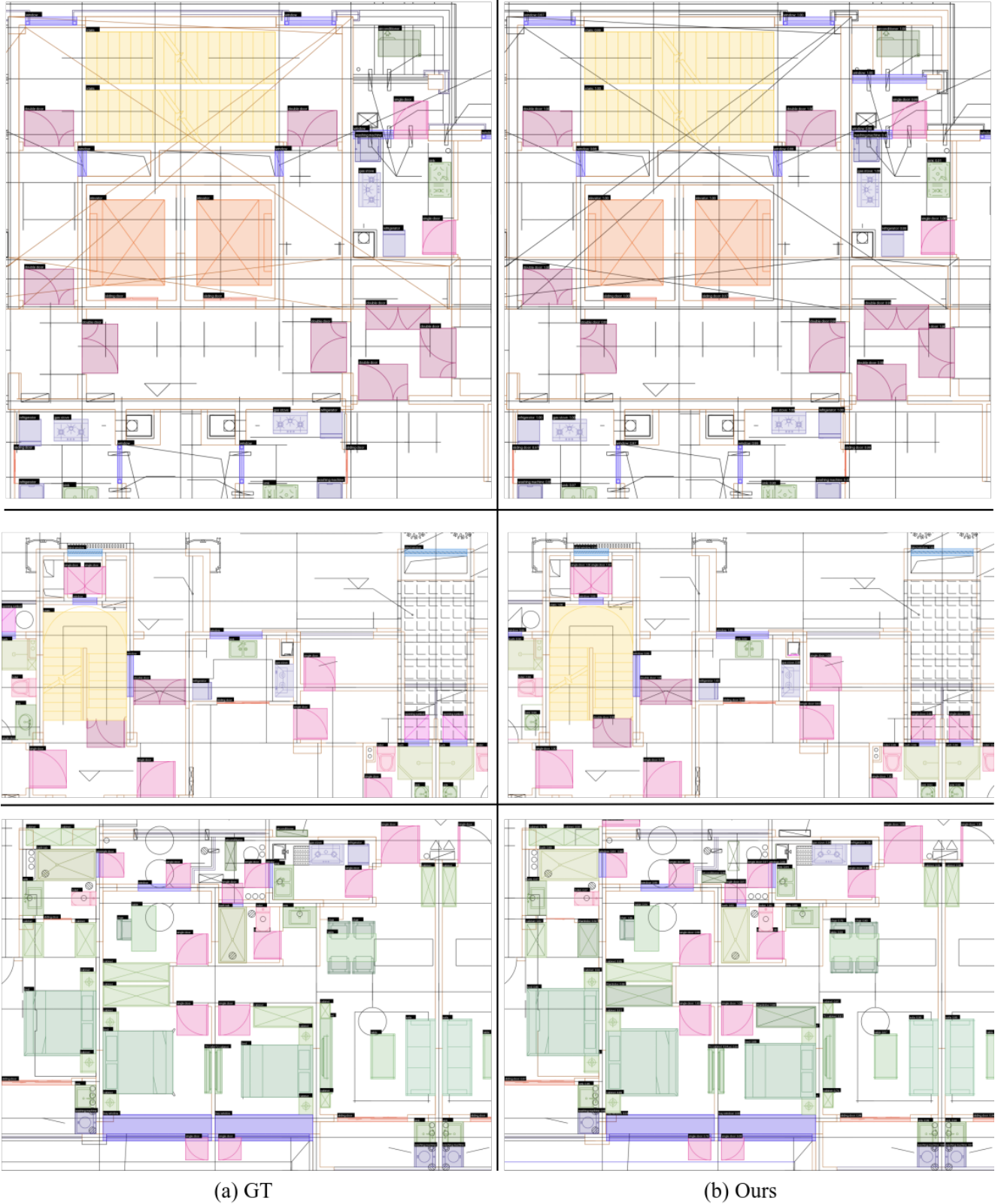


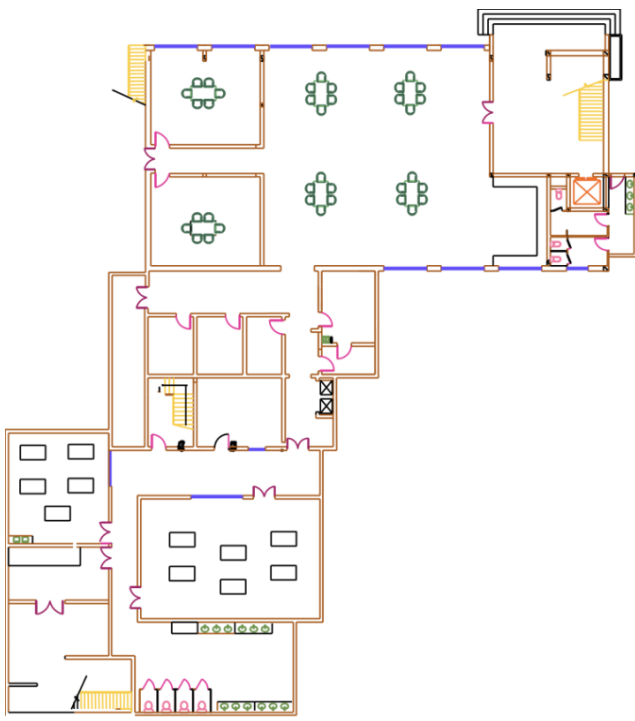
Figure 9. Qualitative comparison of panoptic symbol spotting. Our method accurately detects symbol instances, even in situations where symbols are overlapped by other elements..



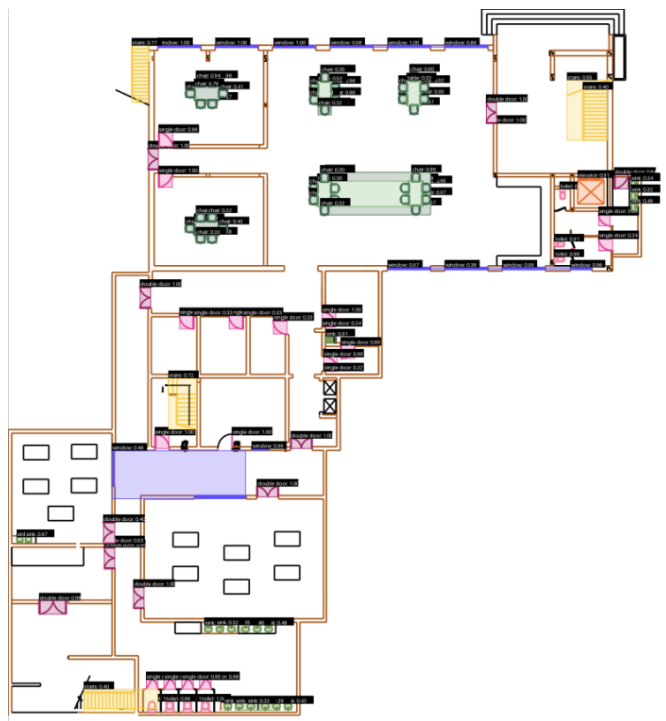
(a) GT

(b) Ours

Figure 10. Qualitative comparison of panoptic symbol spotting. Our method accurately detects symbol instances, even in situations where symbols are overlapped by other elements.

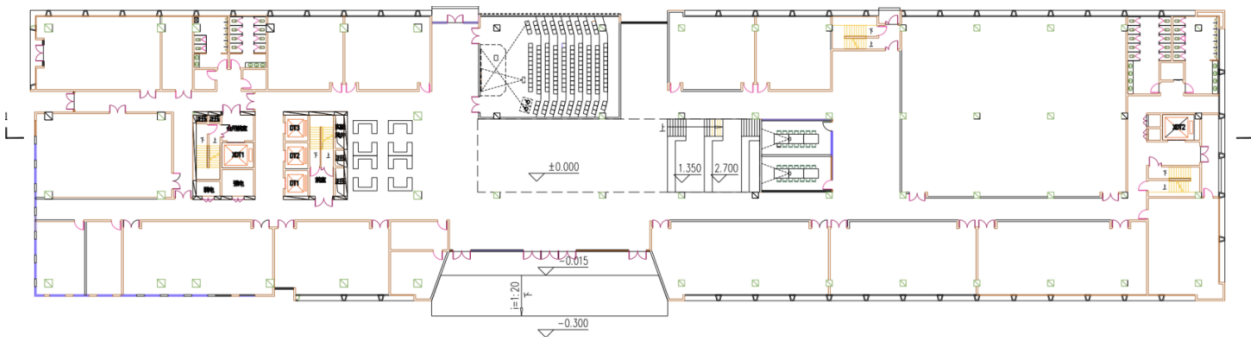


(a) Semantic Pred

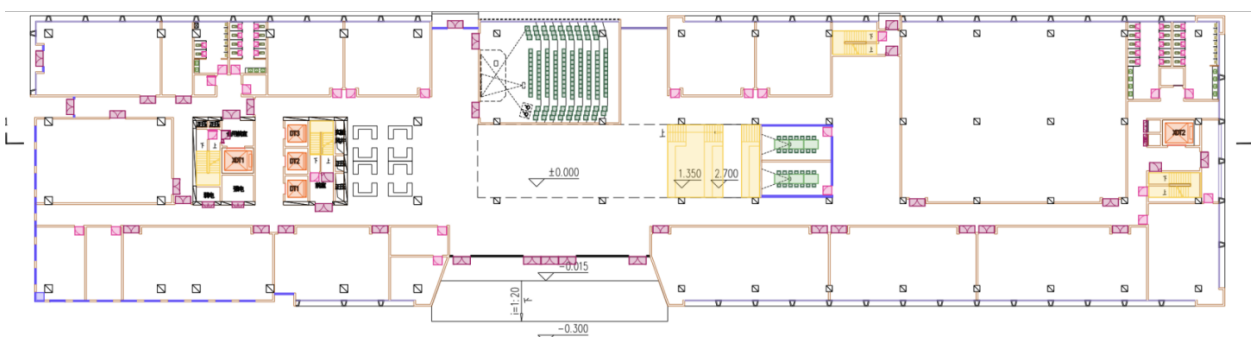


(b) Panoptic Pred

Figure 11. Qualitative visualization highlighting the performance of our method for panoptic symbol spotting on the LS-CAD dataset.



(a) Semantic Pred



(b) Panoptic Pred

Figure 12. Qualitative visualization highlighting the performance of our method for panoptic symbol spotting on the LS-CAD dataset.